Adipose-derived mesenchymal stem cell exosomes inhibit transforming growth factor-β1-induced collagen synthesis in oral mucosal fibroblasts

JUNJIE LIU[1,2*], FUXINGZI LI[3*], BINJIE LIU[1], ZHIGANG YAO[1], LONG LI[1], GUI LIU[1,2], LEI PENG[4], YUXIN WANG[5] and JUNHUI HUANG[1,2]

[1]Hunan Key Laboratory of Oral Health Research; [2]Hunan 3D Printing Engineering Research Center, Hunan Xiangya Stomatological Hospital, Central South University, Changsha, Hunan 410000; [3]Department of Endocrinology and Metabolism, Second Xiangya Hospital, Central South University, Changsha, Hunan 410011, P.R. China; [4]Department of Urban Palliative Home Care, Grey Nuns Community Hospital, Edmonton, AB T5J3E4, Canada; [5]Department of Stomatology, Changsha Central Hospital, Changsha, Hunan 410018, P.R. China

Received December 5, 2020; Accepted May 12, 2021

DOI: 10.3892/etm.2021.10854

Abstract. Oral submucosal fibrosis (OSF) is a potentially malignant oral disorder that requires the further development of advanced treatment strategies. TGF-β1 has been reported to be the main trigger for the increased collagen production and reduced activity of matrix degradation pathways in OSF. Exosomes are key mediators of paracrine signaling that have been proposed for direct use as therapeutic agents for tissue repair and regeneration. The present study aimed to investigate the effects of human adipose-derived mesenchymal stem cell (ADSC) exosomes (ADSC-Exos) on TGF-β1-treated oral fibroblasts *in vitro* and to unravel the potential underlying mechanism of action. Oral mucosal fibroblasts were obtained from the buccal tissues of patients without OSF during extraction of the third molar. ADSCs were obtained from three healthy female individuals during liposuction procedures. ADSC-Exos were isolated by ultracentrifugation and identified by electron microscopy, nanoparticle tracking and western blotting. Immunofluorescence and immunocytochemistry staining were performed to measure the expression levels of vimentin and α-smooth muscle actin in the fibroblasts. Reverse transcription-quantitative PCR and western blotting were used to determine the expression levels of mRNAs and proteins associated with collagen production. The p38 MAPK activator anisomycin was used to identify the underlying mechanisms of the effects of ADSC-Exos on TGF-β1-induced collagen synthesis in oral mucosal fibroblasts. The results of the present study revealed that ADSC-Exos exhibited a cup- or sphere-shaped morphology, with a mean diameter of 58.01±16.17 nm. ADSC-Exos were also found to be positive for CD63 and tumor susceptibility 101 expression. ADSC-Exos treatment reversed the TGF-β1-induced upregulation of collagen I and III protein expression. In addition, in the presence of TGF-β1, the expression levels of collagen type I α 1 chain and collagen type III α 1 chain mRNA were downregulated, whilst the expression levels of matrix metalloproteinase (MMP)1 and MMP3 were upregulated following ADSC-Exos treatment. The TGF-β1-induced upregulation in the phosphorylation of p38 in addition to the increased protein expression of collagens I and III were also reversed in fibroblasts following ADSC-Exos treatment. However, anisomycin treatment alleviated these ADSC-Exos-induced changes. In conclusion, findings from the present study suggest that ADSC-Exos may represent a promising strategy for OSF treatment by targeting the p38 MAPK signaling pathway.

Correspondence to: Professor Junhui Huang, Hunan 3D Printing Engineering Research Center, Hunan Xiangya Stomatological Hospital, Central South University, 72 Xiangya Road, Changsha, Hunan 410000, P.R. China
E-mail: 808003@csu.edu.cn

*Contributed equally

Key words: adipose-derived mesenchymal stem cell exosomes, fibroblasts, TGF-β1, collagen synthesis, oral submucous fibrosis

Introduction

Oral submucous fibrosis (OSF) is a potentially malignant oral condition that has been extensively studied (1). In particular, Pindborg and Sirsat were the first to propose that OSF may be a precancerous condition in 1966 (2). The malignant transformation rate of patients with OSF ranges from 1.2 to 23% worldwide and according to statistics, OSF has a high tendency to develop into oral cancer 3-16 years after OSF diagnosis (3). At present, accumulating evidence has indicated that chewing of areca nut is recognized as one of the most important risk factors for OSF (4,5).

It has been frequently reported that TGF-β1 induces the phenotypic transformation of fibroblasts into activated fibroblasts (6). A previous study has revealed that TGF-β1 signaling was not only an important suppressor of inflammation and

epithelial cell proliferation, but also a driver of collagen deposition during lung fibrosis (7). TGF-β was suggested to be the main trigger for the increased collagen production and decreased activity of extracellular matrix (ECM) degradation during OSF (8). An increasing number of studies have also shown that the aberrant activation of TGF-β1 signaling can led to the development of OSF (9,10). Pant *et al* (11) previously found that chewing of the areca nut induced the JNK/activating transcription factor 2 (ATF2)/c-Jun signaling axis through activation of the TGF-β signaling pathway in epithelial cells. Therefore, it remains a priority to determine the molecular mechanisms downstream of TGF-β1 signaling in OSF to suppress TGF-β1-induced collagen production, which has been proposed to be a viable treatment strategy for OSF (9). The present study established an *in vitro* TGF-β1-induced cell model, similar to that reported in previous studies (12-14), to investigate the association between collagen deposition and OSF.

Exosomes are extracellular membrane-enclosed particles that are ~40-150 nm in size and are of endosomal origin, which can contain microRNAs (miRNAs/miR), RNAs and proteins (15,16). Exogenous exosomal molecules are important mediators of paracrine signaling, which regulate recipient cell function by transferring information that can regulate the expression of specific genes or proteins (17,18). Previous studies have reported the use of adipose-derived mesenchymal stem cell (ADSC) exosomes (ADSC-Exos) for treating fibrotic diseases, including liver fibrosis (19,20), kidney fibrosis (21) and for the formation of scars during skin wound healing (22). Although OSF is a disease that appears to be caused by excessive collagen deposition and dysregulation of ECM remodeling (23), to the best of our knowledge the effect of ADSC-Exos on OSF remains unclear.

The present study isolated exosomes from human ADSCs and investigated the possible biological role of ADSC-Exos on oral mucosal fibroblasts following TGF-β1 stimulation. In particular, the effects of ADSC-Exos on the expression levels of collagen type I α 1 chain (COL1A1), collagen type III α 1 chain (COL3A1), matrix metalloproteinase (MMP)1 and MMP3 in addition to the production of collagen in TGF-β1-induced oral mucosal fibroblasts were determined. Furthermore, the present study also explored the possible underlying mechanism of the role of ADSC-Exos in collagen metabolism.

Materials and methods

Ethics statement. All individuals provided written informed consent prior to participation in the present study and the study protocol was approved by the Ethics Committee of Hunan Xiangya Stomatological Hospital affiliated with Central South University (approval no. 20190015; Changsha, China).

Isolation of oral fibroblasts and ADSCs. Oral mucosal fibroblasts were obtained from the buccal tissues of patients without OSF during extraction of the third molar in April-May 2019 at Hunan Xiangya Stomatological Hospital, Central South University. The inclusion criteria were as follows: i) Patients agreed to provide tissue samples to be analyzed in the present study; ii) provided written informed consent; iii) aged ≥18 years; and iv) no systemic diseases. The exclusion criteria were as follows: i) Areca-chewers; ii) smokers; and iii) oral mucosal diseases, including leukoplakia and lichen planus. The patients were comprised two men and one woman, with an age 26.00±1.63 years. Fibroblasts were cultured and maintained according to a previously described method (24,25). Briefly, the submucosal tissue was obtained from the buccal mucosa for primary culture. The tissue was washed three times with ice-cold PBS containing 20% penicillin/streptomycin mixture before the epithelial tissue was removed under aseptic conditions. The tissues were then cut into small pieces (0.5x0.5x0.5 mm) and washed with RPMI-1640 medium (Hyclone; Cytiva) supplemented with 10% FBS (Gibco; Thermo Fisher Scientific, Inc.). In total, five times the amount of collagenase II (Gibco; Thermo Fisher Scientific, Inc.) was added to the tissue mass at a concentration of 2 mg/ml and digested for 30 min in a 37˚C incubator. Subsequently, 3-5 ml RPMI-1640 complete medium was added to terminate the digestion and the mixture was incubated at room temperature for 5 min. After centrifugation at room temperature at 300 x g for 10 min, the supernatant was discarded and five times the amount of collagenase II was added to the tissue mass at a concentration of 2 mg/ml for 30 min in a 37˚C incubator. This step was repeated three to four times. After centrifugation at room temperature 300 x g for 10 min, the cells were collected cells again by discarding the supernatant before 5 ml of RPMI-1640 full culture medium was added to the cell pellet and transferred into T25 cell culture flasks. All cells were maintained at 37˚C in an incubator containing 5% CO_2. For the selected experiments, fibroblasts were stimulated with 0, 0.1, 1 and 10 ng/ml recombinant TGF-β1 (PeproTech, Inc.) at 37˚C for 48 h.

ADSCs were obtained from three healthy female individuals (age, 28.67±1.89 years; range, 25-30 years) during liposuction procedures performed at the Plastic Surgery Department of The Xiangya Hospital Central South University in December 2019. Isolation of ADSCs was performed as previously described (26). Briefly, the adipose tissue was cut into small pieces and digested with 0.1% collagenase type II (Gibco; Thermo Fisher Scientific, Inc.) at 37˚C water bath and shaken once every 5 min. After the adipose tissue particles disappear and the liquid reached a uniform state, an equal volume of low glucose-DMEM (L-DMEM; HyClone; Cytiva) complete medium (90% L-DMEM + 10% FBS + 1% penicillin and streptomycin suspension) to terminate the digestion at room temperature. After centrifugation at room temperature 300 x g for 5 min, the supernatant was discarded. The cell pellet was resuspended in 5 ml L-DMEM medium and transferred into culture flasks. ADSCs were cultured in L-DMEM supplemented with 10% FBS, cells were maintained at 37˚C in an incubator containing 5% CO_2.

Identification of ADSCs. To assess the capacity (including osteogenesis and adipogenesis) for ADSCs multilineage differentiation, cells were cultured under differentiating conditions. For adipocyte differentiation, ADSCs were cultured in the adipogenesis induction medium (cat. no. HUXMD-90031; Cyagen Biosciences, Inc.) at 37˚C for 21 days. At the end of the incubation, ADSCs were fixed in 4% paraformaldehyde at room temperature for 30 min and stained with Oil Red O (cat. no. G1262; Beijing Solarbio Science & Technology Co., Ltd.)

at room temperature for 20 min. For osteoblast differentiation, the ADSCs were cultured in osteogenesis induction medium (cat. no. HUXMA-90021; Cyagen Biosciences, Inc.) at 37˚C for 14 days. The osteogenic ADSCs were then fixed in 4% paraformaldehyde at room temperature for 20 min and stained with 2% Alizarin red solution (cat. no. C0140; Beyotime Institute of Biotechnology) at room temperature for 15 min. Stained cells were visualized using a light microscope at x100 magnification (CX31; Olympus Corporation). The expression of surface marker proteins (CD29, CD44, CD73, CD90, CD34 and CD45) on ADSCs was detected by flow cytometry. The ADSCs were harvested and washed twice with PBS before being centrifuged at room temperature at 500 x g for 5 min and the pelleted cells were collected. Then fix the cells in 4% PFA at room temperature for 20 min. The cells were washed twice with 1 ml washing buffer by centrifugation at room temperature at 500 x g for 5 min. The cells were then suspended in 1 ml permeabilization buffer for 10 min at room temperature before being centrifuged at room temperature 500 x g for 5 min and the pellet was collected. The cells were washed again for two times with PBS to the cells before being centrifuged again at room temperature 500 x g for 5 min. The cells were then incubated with 3% BSA (Beyotime Institute of Biotechnology) in PBS for 30 min at room temperature. In total, $1x10^6$ per aliquot of cells in 100 μl blocking buffer were incubated with the following primary antibodies for 45 min at room temperature: Mouse anti-Human CD29 (cat. no. 65191-1-Ig; 1:10; Proteintech Group, Inc.), mouse anti- Human CD44 (cat. no. 65063-1-Ig; 1:10; Proteintech Group, Inc.), mouse anti-Human CD73 (cat. no. 65162-1-Ig; 1:10; Proteintech Group, Inc.), rabbit anti-Mouse CD90 (cat. no. FITC-65088; 1:10; Proteintech Group, Inc), mouse anti-CD34 (cat. no. 60180-1-Ig; 1:10; Proteintech Group, Inc.) and mouse anti-Human CD45 (cat. no. 60287-1-Ig; 1:10; Proteintech Group, Inc.). If using FITC-conjugated primary antibodies, no secondary antibody incubation was used. The cells were then incubated with diluted secondary antibodies (Alexa Fluor® 488-conjugated goat anti-mouse IgG; cat. no. ab150117; 1:25; Abcam) and incubated for 45 min at room temperature in the dark. A separate secondary antibody (Alexa Fluor® 488-conjugated goat anti-mouse IgG or goat anti-rabbit IgG; cat. no. ab150077; 1:25; Abcam) incubation was used as a negative control. Using 5% BSA as the flow cleaning solution, unbound fluorescence and impurities were washed off and the cells were loaded into the BD FACSCanto II (BD Biosciences) flow cytometer for measurements. The results were analyzed using the Flowjo VX10 software (FlowJo LLC).

ADSC-Exos extraction. Exosome extraction was performed as previously described with a number of modifications (22). Briefly, ADSCs were cultured until cells reached 80% confluence. The medium was then replaced with serum-free L-DMEM at 37˚C for 24 h. The conditioned medium was collected and centrifuged at 300 x g for 10 min at 4˚C and then at 2,000 x g for 30 min at 4˚C to remove dead cells and cellular debris. After further centrifugation at 2,000 x g for 30 min at 4˚C, the supernatant containing exosomes was collected. Thereafter, the exosome suspension was filtered through a 0.22-μm filter (EMD Millipore). A total of 15 ml exosome suspension was added to an Amicon® Ultra-15 Centrifugal Filter device unit (100 kDa; EMD Millipore) and the supernatant was collected after centrifugation at 4,000 x g for 1 h at 4˚C. To recover the concentrated solute, a pipettor was inserted into the bottom of the filter device to withdraw the sample using a side-to-side sweeping motion into ensure total recovery. The volume of the ultrafiltration liquid was reduced from 15 to ~1 ml, before 1/5 volume of Exoquick Exosome Precipitation solution (System Bioscience, LLC) was added to the exosome suspension for 12 h at 4˚C. On the next day, the mixture was centrifuged at 4˚C at 1,500 x g for 30 min and the supernatant was removed, before the yellow or beige precipitate at the bottom of the tube was identified as exosomes. Finally, an appropriate amount of PBS (300-500 ml) was added to resuspend the precipitate and the exosome suspension was obtained after the pipetting gun was blown evenly. Exosome concentration was determined using a BCA protein assay kit (Beyotime Institute of Biotechnology).

Identification of ADSC-Exos. The morphology of the exosomes was observed by transmission electron microscopy (TEM), as previously described (27). ADSC-Exos pellets (~5 μl) were fixed with 2.5% glutaraldehyde at room temperature for ≥2 h, washed three times with 0.1 M PBS for 15 min each time and then fixed with 1% osmium acid at room temperature for 1-2 h. The pellets were then dehydrated sequentially in 70, 90 and 100% acetone for 10 min each time. Pure acetone and embedding solution [Embed812; Head (Beijing) Biotechnology, Co., Ltd.] was mixed 1:1 and then added to the exosomes at 37˚C for 12 h, followed by overnight at 37˚C and 24 h at 60˚C for curing. Finally, the exosomes underwent double staining with 3% uranyl acetate and lead nitrate at room temperature for 20-30 min. ADSC-Exos were observed using a Hitachi H-7650 transmission electron microscope (H-7650H; Hitachi, Ltd.). The size distribution of the ADSC-Exos was measured by dynamic light scattering with a Malvern Nano instrument (ZS90; ZEN3690; Malvern Instruments). Expression levels of the characteristic surface marker proteins on the exosomes were extracted using RIPA lysis buffer (Beijing Solarbio Science & Technology Co., Ltd.) and analyzed by western blotting.

Exosome uptake assay. ADSC-Exos were labeled with a green, fluorescent 3,3'-dioctadecyloxacarbocyanine perchlorate (DiO) dye (Thermo Fisher Scientific, Inc.) according to the manufacturer's protocol. Briefly, 1 μl DiO dye (200 μg/ml; Thermo Fisher Scientific, Inc.) was added to 20 μl exosome suspension and incubated for 20 min at 37˚C. The reaction was stopped by the addition of an equivalent volume of exosome-depleted BSA (Sigma-Aldrich; Merck KGaA), before DiO-labeled exosomes were obtained.

Fibroblasts were washed twice with PBS and seeded at a density of $2x10^5$ into six-well plates for 48 h at 37˚C. Next, 50 ng/μl DiO-labeled exosomes were added to the fibroblasts and incubated at 37˚C in the dark for 6 h before being subsequently fixed with 4% paraformaldehyde at room temperature for 15 min. The cells were then incubated with 0.5% Triton X-100 at room temperature for 15 min and blocked with 10% BSA at 37˚C for 30 min. The fibroblasts were then stained with 2.5% phalloidin (cat. no. 40734ES75; Shanghai Yeasen Biotechnology Co., Ltd.) at room temperature for

20 min. After washing with PBS, the nuclei were then stained with DAPI at room temperature for 3 min (0.5 μg/ml; Invitrogen; Thermo Fisher Scientific, Inc.). The fluorescent cells were visualized using a Zeiss LSM 800 confocal microscope at x100 magnification (Zeiss GmbH).

Immunofluorescence assay. Immunofluorescence was used to detect the expression of vimentin under normal condition or following TGF-β1 (10 ng/ml) treatment at 37˚C for 2 days. The experiment was divided into two groups, the control group (PBS) and the experimental group (TGF-β1). Briefly, fibroblasts were first fixed with 4% paraformaldehyde for 15 min at room temperature. After permeabilization with 0.5% Triton X-100/PBS for 15 min at room temperature, non-specific binding was blocked with 5% BSA for 1 h at 37˚C. Cells were subsequently incubated with a rabbit anti-vimentin monoclonal antibody (cat. no. 9782; 1:1,000; Cell Signaling Technology, Inc.) at 4˚C overnight. Following the primary antibody incubation, cells were incubated with an Alexa Fluor® 488-conjugated goat anti-rabbit IgG secondary antibody (cat. no. ab150077; 1:2,000; Abcam) for 1 h at 37˚C. The nuclei were counterstained with DAPI at room temperature for 3 min (0.5 μg/ml; Invitrogen; Thermo Fisher Scientific, Inc.). Stained cells were visualized using a Leica DMI6000B fluorescence microscope at x100 magnification (Leica Microsystems GmbH).

Immunocytochemistry. Immunocytochemistry was used to detect the expression of α-SMA under normal condition and following TGF-β1 (10 ng/ml) treatment at 37˚C for 2 days. The experiment was divided into two groups, the control group (PBS) and the experimental group (TGF-β1). Briefly, fibroblasts were fixed with 4% paraformaldehyde at room temperature for 15 min and then permeabilized with 0.5% Triton X-100/PBS for 15 min at room temperature. Afterwards, 25 μl 1% donkey serum (cat. no. SL050; Beijing Solarbio Science & Technology Co., Ltd.) to each sample at room temperature for 20 min for blocking. Cells were incubated with the rabbit anti-α smooth muscle actin (SMA) antibody (cat. no. ab124964; 1:2,000; Abcam) for 2 h at 37˚C. Enhanced enzyme-labeled goat anti-mouse/rabbit IgG polymer (cat. no. PV-9000; ZSGB-BIO; OriGene Technologies, Inc.) was then added and incubated at room temperature for 30 min. DAB (cat. no. DA1015; Beijing Solarbio Science & Technology Co., Ltd.) color developing solution was added and incubate for 2 min at room temperature. Hematoxylin (Beijing Solarbio Science & Technology Co., Ltd.) counterstain was then used for 1 min at room temperature. Stained cells were visualized using light microscopy at x100 magnification (CX31; Olympus Corporation).

Western blotting. Firstly, the fibroblasts were divided into four concentration groups: 0, 0.1, 1 and the 10 ng/ml TGF-β1 groups. In addition, the fibroblasts were divided into three groups: 10 μg/ml TGF-β1 + 100 μg/ml ADSC-Exos, negative control (PBS) and positive control group (TGF-β1). The fibroblasts were also divided into four groups and incubated for 30 min at 37˚C: 10 ng/ml TGFβ1 + 100 μg/ml ADSC-Exos; 10 ng/ml TGF-β1 + 100 μg/ml ADSC-Exos + 25 μg/ml Anisomycin (Cell Signaling Technology, Inc.); 10 ng/ml TGF-β1 and 10 ng/ml TGFβ1 + 25 μg/ml Anisomycin.

Total protein was extracted from fibroblasts and exosomes using RIPA lysis buffer (Beijing Solarbio Science & Technology Co., Ltd.). The protein was lysed on ice for 30 min, centrifuged at 12,000 x g at 4˚C for 10 min and the supernatant was removed. A 20 μl sample was taken for protein concentration determination by BCA method. Proteins (40 μg per lane) were separated using 10% SDS-PAGE. The separated proteins were subsequently transferred onto polyvinylidene fluoride membranes (EMD Millipore) and blocked with 5% non-fat milk or 5% BSA at room temperature for 60 min. Membranes were then incubated with the following primary antibodies at 4˚C overnight: Mouse anti-phosphorylated (p)-p38 (cat. no. sc-7973; 1:200; Santa Cruz Biotechnology, Inc.), rabbit anti-p38 (cat. no. sc-535; 1:200; Santa Cruz Biotechnology, Inc.), mouse anti-CD63 (cat. no. sc-5275; 1:500; Santa Cruz Biotechnology, Inc.), rabbit anti-collagen I (cat. no. 14695-1-AP; 1:1,000; ProteinTech Group, Inc.), rabbit anti-tumor susceptibility 101 (TSG101; cat. no. 14497-1-AP; 1:1,000; ProteinTech Group, Inc.), rabbit anti-collagen III (cat. no. C7805; 1:2,000; Sigma-Aldrich; Merck KGaA) and rabbit anti-GAPDH (cat. no. GB11002; 1:2,000; Wuhan Servicebio Technology Co., Ltd.). Following the primary antibody incubation, the membranes were incubated with HRP-conjugated anti-rabbit IgG (cat. no. 7074; 1:5,000; Cell Signaling Technology, Inc.) or anti-mouse IgG (cat. no. 7076; 1:5,000; Cell Signaling Technology, Inc.) secondary antibodies at 37˚C for 1 h. Protein bands were visualized using enhanced chemiluminescence reagent (Thermo Fisher Scientific, Inc.) and analyzed using the Image Lab V3.0 (Bio-Rad, Laboratories, Inc.).

Reverse transcription-quantitative PCR (RT-qPCR). After 2 days of 100 μg/ml ADSC-Exos intervention at 37˚C, fibroblasts were extracted and detected to detect the expressions of collagen-synthesis-related genes COL1A1 and COL3A1 and metalloproteinase genes MMP1 and MMP3. Total RNA was extracted from fibroblasts using TRIzol Reagent (Invitrogen; Thermo Fisher Scientific, Inc.) as previously described (28). RNA concentration was detected using a NanoDrop ND-1000 spectrophotometer (Thermo Fisher Scientific, Inc.) at wavelengths of 260 and 280 nm. In total, 1 μg RNA from each sample was reverse transcribed into cDNA using a Revert Aid First Strand cDNA Synthesis kit (Fermentas; Thermo Fisher Scientific, Inc.). The temperature protocol used was pre-denaturation at 70˚C for 5 min, followed by 25˚C for 5 min, 42˚C for 60 min and inactivation at 70˚C for 5 min. qPCR was subsequently performed using SYBR® Premix Ex Taq™ II system (cat. no. DRR820A; Takara Bio, Inc.) on an ABI PRISM® 7900HT system (Applied Biosystems; Thermo Fisher Scientific, Inc.). The following thermocycling conditions were used for the qPCR: 95˚C pre-denaturation 60 sec, followed by 40 cycles at 95˚C denaturation 15 sec, 60˚C annealing 15 sec and 72˚C extension 45 sec. The following primer sequences (Sangon Biotech Co., Ltd.) were used for the qPCR: COL1A1 forward, 5'-ATCAACCGGAGGAATTTCCGT-3' and reverse, 5'-CAC CAGGACGACCAGGTTTTC-3'; COL3A1 forward, 5'-GCC AAATATGTGTCTGTGACTCA-3' and reverse, 5'-GGGCGA GTAGGAGCAGTTG-3'; MMP1 forward, 5'-GGCTGAAAG TGACTGGGAAACC-3' and reverse, 5'-TGCTCTTGGCAAA TCTGGCGTG-3'; MMP3 forward, 5'-CTGGACTCCGACAC TCTGGA-3' and reverse, 5'-CAGGAAAGGTTCTGAAGTG

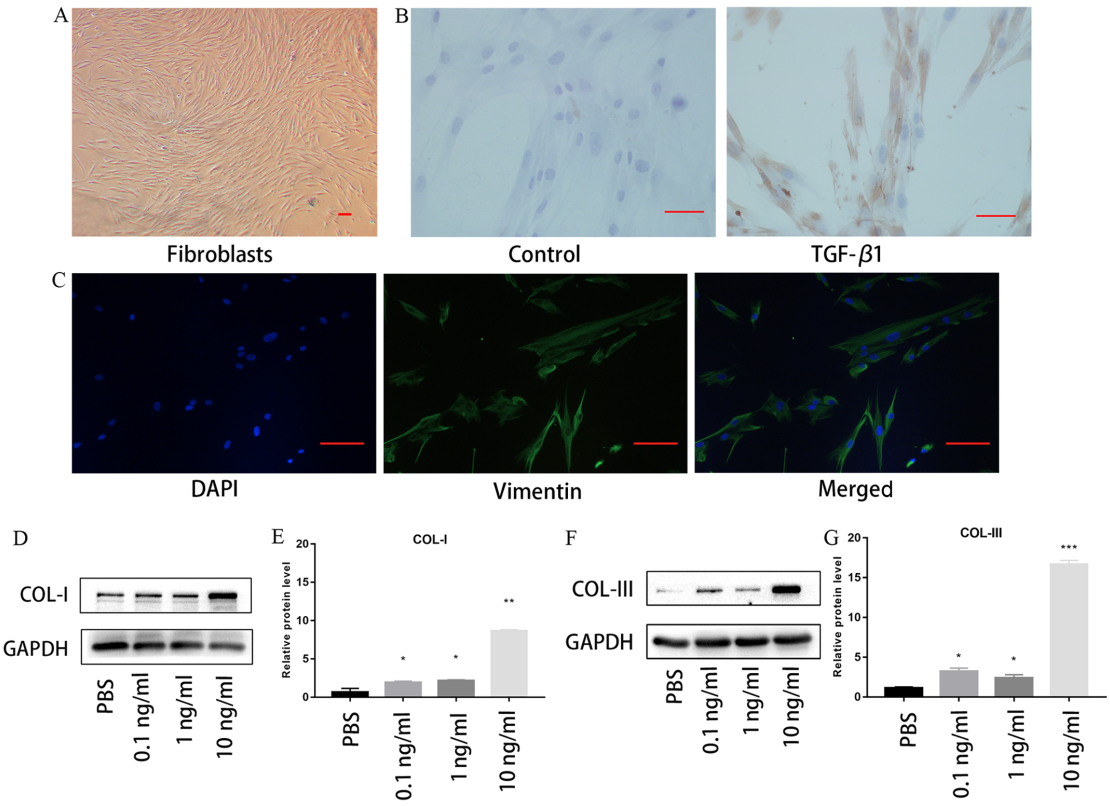

Figure 1. TGF-β1 induces collagen production in oral mucosal fibroblasts. (A) Oral fibroblasts exhibited a spindle-like morphology without TGF-β1 treatment. (B) Immunocytochemistry staining for α-SMA expression in fibroblasts with (10 ng/ml) or without TGF-β1 treatment. (C) Vimentin expression was analyzed using immunofluorescence staining (green) without TGF-β1 treatment. Scale bars, 100 μm. (D-G) Western blotting analysis revealed that TGF-β1 treatment upregulated the expression levels of (D) collagen I and (E) III. The results are presented as the mean ± SD; n=3 for each group. *P<0.05, **P<0.01 and ***P<0.001 vs. PBS. α-SMA, α-smooth muscle actin; COL, collagen.

ACC-3' and GAPDH forward, 5'-GGCACAGTCAAGGCTG AGAATG-3' and reverse, 5'-ATGGTGGTGAAGACGCCA GTA-3'. Relative gene expression was calculated using the $2^{-\Delta\Delta Cq}$ method (29). GAPDH was used as the housekeeping gene for normalization.

Statistical analysis. Data analysis was performed using the SPSS 20.0 software (IBM Corp.). Data are presented as the mean ± SD. Statistical differences between two groups were determined using an unpaired Student's t-test and comparisons among multiple groups were performed using a one-way analysis of variance followed by Tukey's post hoc test. P<0.05 was considered to indicate a statistically significant difference.

Results

TGF-β1 induces collagen production in oral mucosal fibroblasts. Oral mucosal fibroblasts were found to exhibit a spindle-like morphology without TGF-β1 treatment (Fig. 1A). Immunocytochemistry staining revealed that positive staining for α-SMA, a marker of myofibroblasts, was markedly increased following 10 ng/ml TGF-β1 stimulation (Fig. 1B). Immunofluorescence staining demonstrated that vimentin was expressed by the fibroblasts without TGF-β1 treatment (Fig. 1C). Fibroblasts were also treated with 0, 0.1, 1 or 10 ng/ml TGF-β1 for 48 h. As shown in Fig. 1D and E, the expression levels of collagen I and III were significantly upregulated by TGF-β1 in the oral mucosal fibroblasts in a concentration-dependent manner, compared with those in cells treated with PBS. Notably, the expression levels of collagen I and III were the highest following stimulation with 10 mg/ml TGF-β1. These results indicated that TGF-β1 may increase the synthesis of collagen *in vitro*. Therefore, 10 ng/ml TGF-β1 was used to induce the oral fibroblasts for the following experiments.

Characterization of ADSCs and ADSC-Exos. ADSCs were found to exhibit a spindle-like morphology (Fig. 2A). Following osteogenic or adipogenic medium incubations, the ADSCs were able to differentiate into osteoblasts or adipocytes, as demonstrated by Alizarin Red S and Oil Red O staining, respectively (Fig. 2B and C). Flow cytometry analysis revealed that ADSCs were highly positive for MSC surface markers (17), including CD29, CD44, CD73 and CD90, but negative for CD34 and CD45 (Fig. 2D). TEM and western blotting were used to characterize the exosomes derived from ADSCs. The vesicles exhibited a cup- or sphere-shaped morphology (Fig. 2E), with a mean diameter of 58.01±16.17 nm (Fig. 2F). Western blot analysis revealed that the expression levels of the exosomal marker proteins, CD63 and TSG101 (17), were enriched in ADSC-Exos (Fig. 2G).

ADSC-Exos inhibit TGF-β1-induced collagen production in oral mucosal fibroblasts. As shown in Fig. 3A, the DiO-labeled ADSC-Exos (green, fluorescent dye) were incorporated mainly to the perinuclear regions of phalloidin-labeled

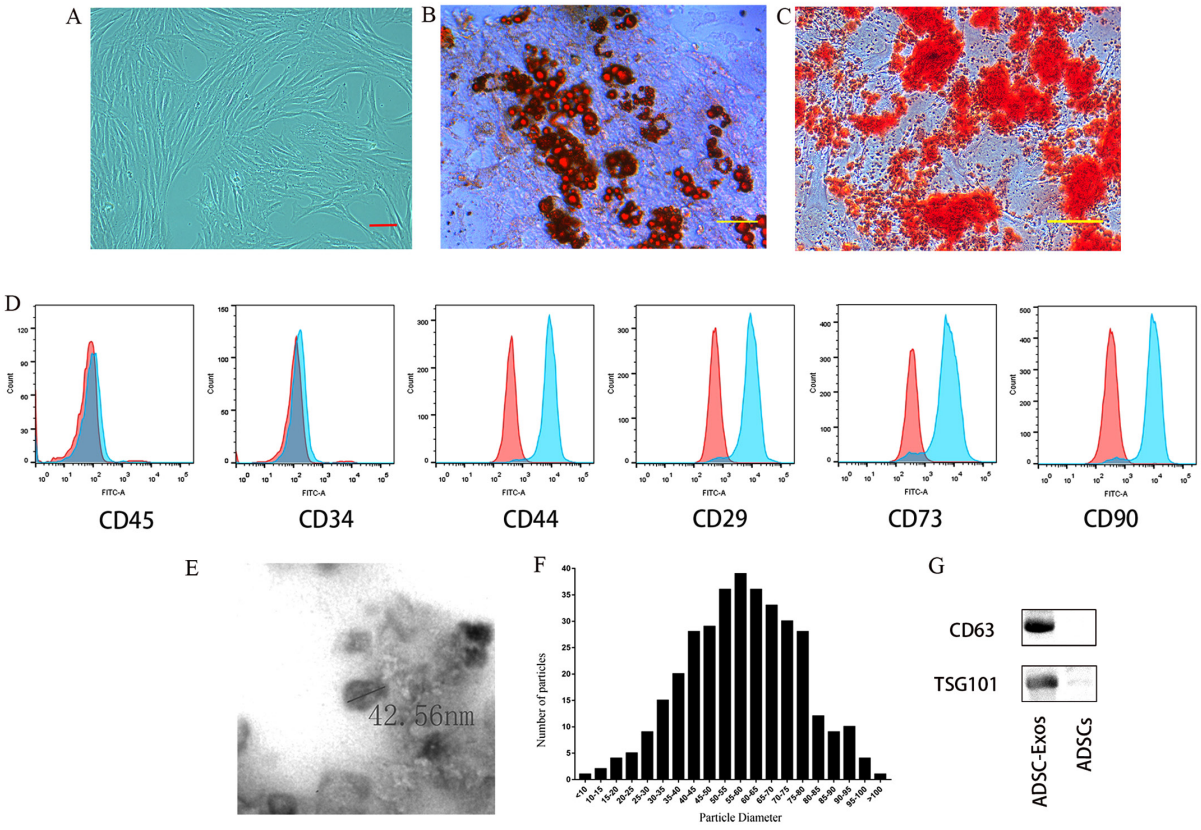

Figure 2. Characterization of the human ADSCs and ADSC-Exos. (A) ADSCs exhibited a spindle-like morphology. (B) Adipogenic and (C) osteogenic differentiation were analyzed using Oil Red O and Alizarin Red S staining, respectively. (D) Flow cytometry analysis of the cell surface markers on ADSCs. (E) Morphology of ADSC-Exos under TEM. (F) Sizes of ADSC-Exos (mean, 58.01±16.17 nm) were calculated from the TEM images. (G) Expression of exosomal surface markers CD63 and TSG101 were detected. TEM, transmission electron microscopy; ADSCs, adipose-derived mesenchymal stem cells; Exos, exosomes; TSG101, tumor susceptibility 101.

fibroblasts (red fluorescent dye). The expression levels of collagen I and III were significantly downregulated in the fibroblasts in the 10 ng/ml TGF-β1 + 100 μg/ml ADSC-Exos group compared with those in the fibroblasts incubated with TGF-β1 alone (Fig. 3B and C).

The expression levels of COL1A1 and COL3A1 mRNA were also found to be significantly downregulated in fibroblasts stimulated with TGF-β1 + ADSC-Exos compared with those in fibroblasts stimulated with TGF-β1 alone (Fig. 3D and E). In addition, when the fibroblasts were stimulated with TGF-β1 + ADSC-Exos, the expression levels of MMP1 and MMP3 were found to be significantly upregulated compared with those in fibroblasts incubated with TGF-β1 alone (Fig. 3F and G).

ADSC-Exos downregulate collagen expression by inhibiting the p38 MAPK signaling pathway. As shown in Fig. 4A, western blotting analysis demonstrated that ADSC-Exos downregulated the phosphorylation levels of p38. The expression levels of collagen I and III were also discovered to be downregulated concomitantly (Fig. 4A). Subsequently, the cultured fibroblasts were treated with 25 μg/ml anisomycin, a p38 activator, in the presence of TGF-β1. As shown in Fig. 4B, anisomycin treatment (TGF-β1 + A) could upregulate the phosphorylation levels of p38 compared with those in fibroblasts stimulated with TGF-β1 alone. The expression levels of collagen I and III were also upregulated following the addition of anisomycin to the medium compared with those in fibroblasts stimulated with TGF-β1 alone (Fig. 4B and C). Notably, ADSC-Exos treatment (TGF-β1 + Exos + A) significantly reversed the effects of anisomycin on p38 phosphorylation and collagen I and III expression.

Discussion

OSF is a multifactorial disease that is caused by the chewing of areca nuts (Fig. 5). According to reports, in 1970 ~10% of the world's population habitually chewed areca nuts (30), but this percentage increased to 10-20% in 2002 (31). In 1996, worldwide estimates indicated that ~2.5 million individuals were affected by OSF (32). Excessive collagen accumulation and hyalinization in the lamina propria, submucosa and superficial muscle layers of the connective tissue are characteristics of OSF (33). Since it has been recognized as one of the oral potentially malignant disorders (5,34), it is important to prevent malignant transformation in patients diagnosed with OSF.

Kondaiah *et al* (35) revealed that areca nut can induce and activate TGF-β in oral epithelial cells, leading to a sustained expression of this profibrotic cytokine, which acts on the fibroblasts and results in OSF. Previous studies have revealed that the aberrant expression of TGF-β1 can lead to the development of a variety of fibrotic diseases, including liver, cardiac and pulmonary fibrosis (36-38). The fibrotic process underlying OSF also involves excessive collagen deposition

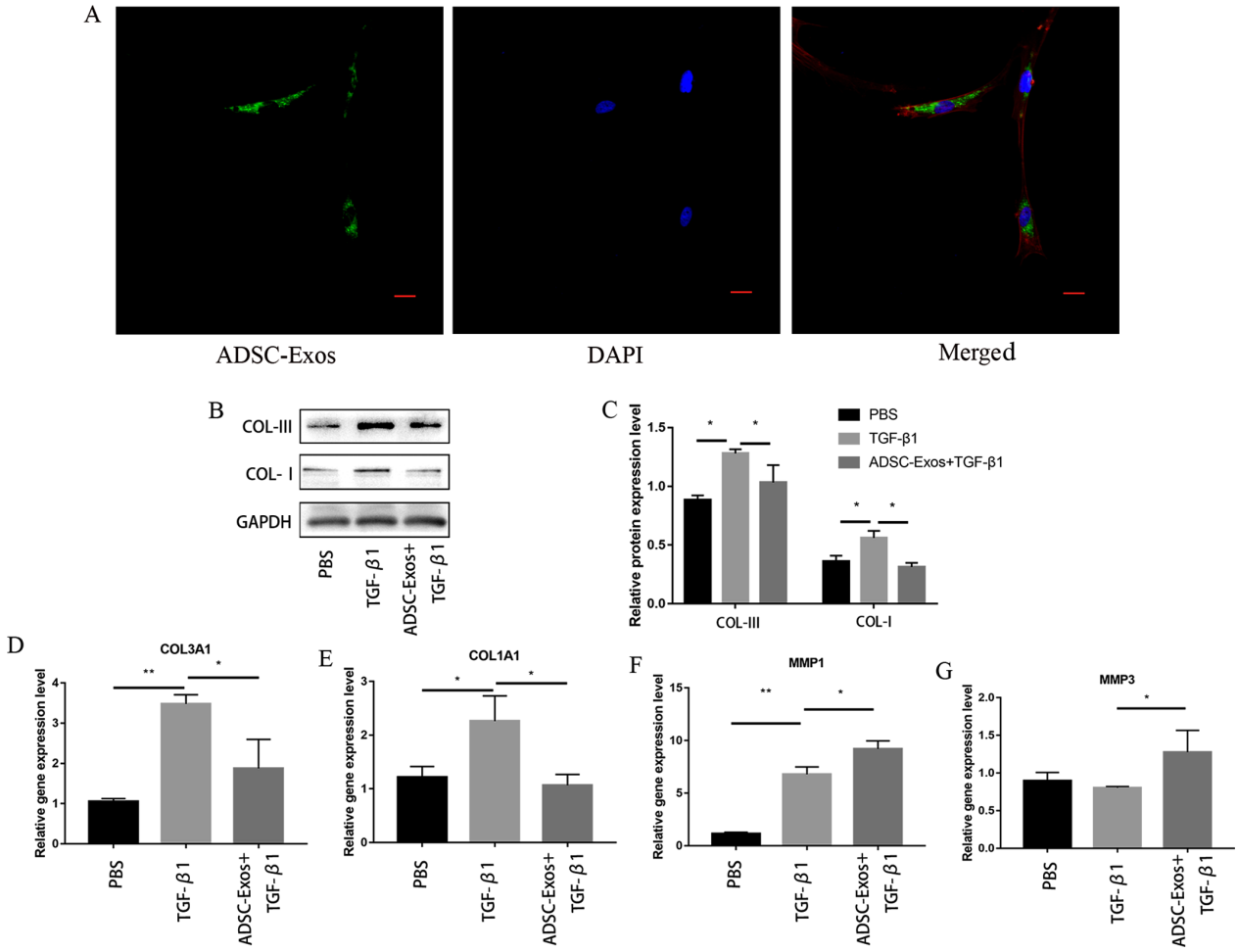

Figure 3. ADSC-Exos inhibit TGF-β1-induced collagen production. (A) Confocal microscopy images of the uptake of DiO-labeled ADSC-Exos by fibroblasts. Green, DiO; red, phalloidin; blue, DAPI. Scale bar, 20 μm. (B) ADSC-Exos downregulated the expression levels of collagen I and collagen III in TGF-β1-induced oral fibroblasts, (C) which was quantified. The mRNA expression levels of (D) COL3A1, (E) COL3A1, (F) MMP1 and (G) MMP3 were analyzed using reverse transcription-quantitative PCR. The results are presented as the mean ± SD; n=3 for each group. *P<0.05 and **P<0.01. ADSC-Exos, adipose-derived mesenchymal stem cells exosomes; DiO, 3,3'-dioctadecyloxacarbocyanine perchlorate; COL1A1, collagen type I α 1 chain; COL3A1, collagen type III α 1 chain; MMP, matrix metalloproteinase.

and dysregulation in the ECM remodeling process (23). ECM components, such as collagen, have been suggested to hold potential as markers for evaluating the severity of OSF (39). Therefore, it can be hypothesized that therapeutically targeting the TGF-β1 signaling pathway and inhibiting the active secretion of collagens may represent a promising approach. Notably, a number of antifibrotic strategies have been previously attempted to target the activation, proliferation and/or recruitment of fibroblasts, including Pirfenidone (40) and Salvia miltiorrhiza Bunge (41). The findings of the present study revealed that the expression levels of α-SMA were upregulated in TGF-β1-induced oral fibroblasts, which is a similar finding to that observed in patients with clinical OSF (35). In addition, the expression levels of collagen I and III were upregulated in cells stimulated with TGF-β1 in a dose-dependent manner. These findings suggested that TGF-β1 can significantly promote the production of collagen in oral fibroblasts.

Mesenchymal stem cells, which have the capacity for self-renewal and differentiation into chondrocytes, osteoblasts and adipocytes (21), can be isolated and expanded from a variety of tissues, including adipose tissues, bone marrow, the umbilical cord and dental pulps (42). Due to their minute size, exosomes confer high hemocompatibility, good stability and do not obstruct the vasculature as a therapeutic agent (43,44). The use of exosomes has been reported to be an effective strategy for immune rejection to kill tumor cells and change the microenvironment for cancer development (45,46). In addition, the role of exosomes in prostate cancer progression and metastasis has been attracting the attention of researchers, with a previous study reporting their potential application as biomarkers and therapeutic targets (47). The present study isolated ADSCs from human adipose tissues, which were able to differentiate into osteocytes and adipocytes under *in vitro* conditions. In the presence of TGF-β1, treatment with ADSC-Exos significantly downregulated the expression levels of collagen I and III. Additionally, the present study suggested that ADSC-Exos also downregulated the expression levels of COL1A1 and COL3A1 mRNA, whilst upregulating those of MMP1 and MMP3 in TGF-β1-induced fibroblasts. These results suggest that ADSC-Exos may not only inhibit collagen expression, but may also promote the degradation of collagen.

Exosomes can contain both mRNA and miRNA and be delivered to other cells in a new location to regulate their function (48). For example, Qu *et al* (20) previously found that

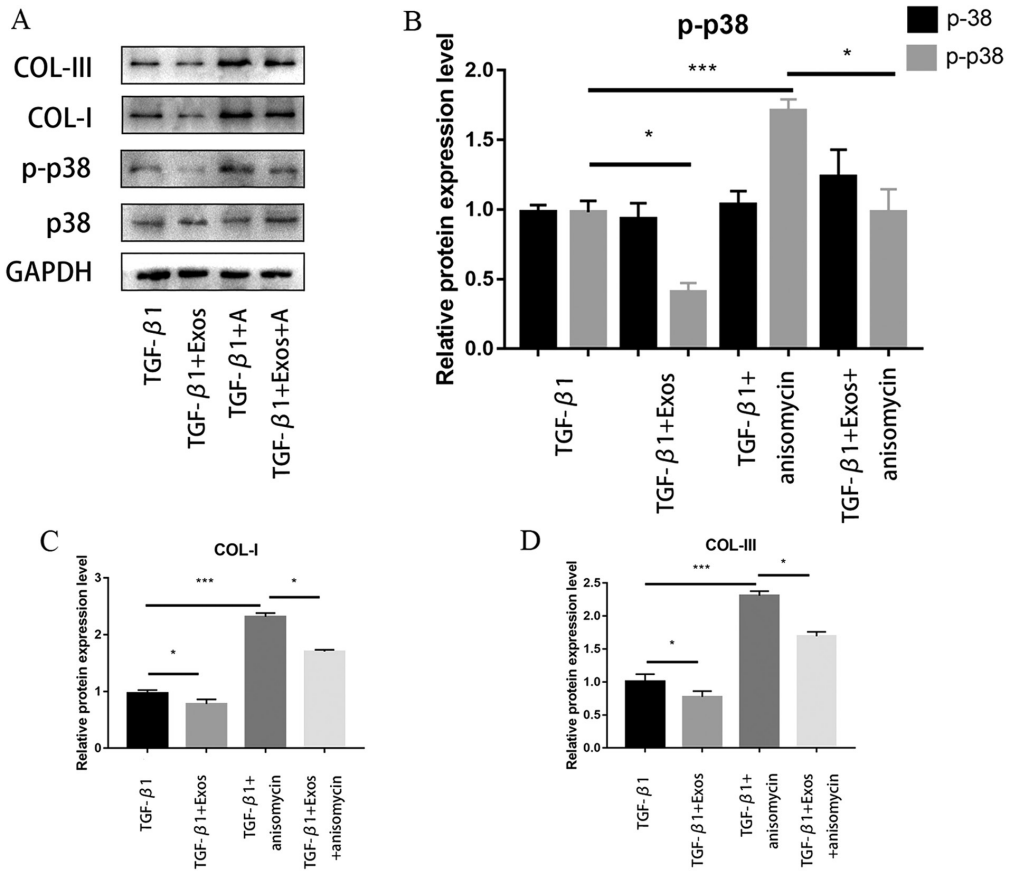

Figure 4. ADSC-Exos downregulate collagen expression by inhibiting p38 MAPK activity. (A) Representative western blotting image showing the protein expression levels of collagen I, collagen III and p38, in addition to the phosphorylation levels of p38 in fibroblasts that were stimulated with TGF-β1 in the presence of anisomycin. Band densities of (B) p38, p-p38, (C) Collagen I and (D) collagen III were quantified. The results are presented as the mean ± SD; n=3 for each group. *P<0.05 and ***P<0.001. p-, phosphorylated; A, anisomycin; ADSC-Exos, adipose-derived mesenchymal stem cells exosomes; COL, collagen.

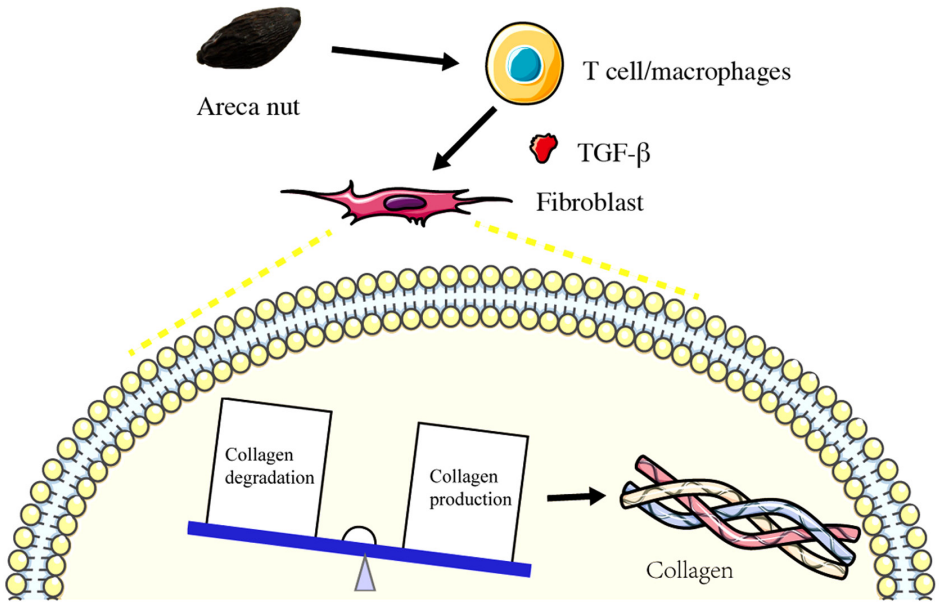

Figure 5. Proposed model of the pathogenesis of OSF. Overproduction of insoluble collagen and reduced degradation of collagen caused by the habit of areca nut chewing and subsequent stimulation of the TGF-β signaling pathway increases collagen deposition in the oral submucosa, which leads to OSF. OSF, oral submucous fibrosis.

ADSC-Exos containing miR-181-5p can increase autophagy and reduce TGF-β1-induced liver fibrosis in hepatic stellate cells in a carbon tetrachloride-induced liver fibrosis mouse model. Pant *et al* (11) found that chewing of the areca nut induced

the JNK/ATF2/c-Jun axis through activation of the TGF-β signaling pathway in OSF. Illeperuma *et al* (49) found that the TGF-β1 expression levels were upregulated in 42 patients with OSF compared with those in the normal oral mucosa and reported that dysregulations in both collagen deposition and degradation occurred during the fibrosis process. In addition, ADSC-Exos have been reported to be internalized by fibroblasts, leading to the upregulation of the gene expression levels of N-cadherin, cyclin D1, collagen I and collagen III, thereby increasing wound healing (50). Another previous study has also reported the promising effects of applying ADSC-Exos for accelerating wound healing, where they deliver miR-21 to the fibroblasts and downregulate TGF-β1 protein expression, thereby reducing the formation of scars (51). Therefore, there is experimental evidence that ADSC-Exos can regulate the expression of collagen, though the specific underlying mechanism remain a topic for further research.

The p38 MAPK signaling pathway has been closely associated with collagen synthesis, which promotes ECM production (52). Li *et al* (52) found that ADSC-conditioned medium can decrease collagen deposition of fibroblasts by regulating the p38/MAPK signaling pathway. Similarly, Chai *et al* (53) also reported that ADSC-conditioned medium can decrease collagen deposition and suppress scar formation by inhibition of the p38 MAPK signaling pathway. Consistent with these previous findings, results from the present study demonstrated that ADSC-Exos can downregulate the levels of p38 phosphorylation and collagen I and III expression in oral fibroblasts following TGF-β1 stimulation. However, following the treatment with anisomycin, a p38 activator, the phosphorylation levels of p38 and the expression levels of collagen I and III were upregulated. These observations suggested that inhibition of the p38 MAPK signaling pathway may serve a key role in the antifibrotic properties of ADSC-Exos.

From the present study, the underlying mechanism through which ADSC-Exos exert their effects on the fibroblasts requires further investigation. A limitation of present study is that the effect of ADSC-Exos was not investigated using *in vivo* experiments and the lack of investigations in the effects potentially mediated by TGF-β2 and 3, both of which also warrant further investigation.

In conclusion, findings of the present study demonstrated that ADSC-Exos can inhibit TGF-β1-induced collagen synthesis in oral mucosal fibroblasts *in vitro* by regulating the p38 MAPK signaling pathway. Therefore, the application of ADSC-Exos may represent a promising strategy for OSF treatment.

Acknowledgements

Not applicable.

Funding

The present study was supported by funding from The Hunan 2018 Key R & D Project of China (grant no. 2018SK2104), China Hunan Provincial Science and Technology Program (grant no. 2017GK2265) and The Fundamental Research Funds for the Central Universities of Central South University (grant no. 2018zzts918).

Availability of data and materials

The datasets used and/or analyzed during the current study are available from the corresponding author on reasonable request.

Authors' contributions

JL and FL performed all the experiments and analyzed the data. BL, ZY, LL, YW and GL contributed to data acquisition and performed statistical analysis. LP revised the manuscript for important intellectual content, made substantial contributions to conception and design, gave final approval of the version to be published, and agreed to be accountable for all aspects of the work. JH designed the study. JL and JH confirm the authenticity of the raw data. All authors read and approved the final version of the manuscript.

Ethics approval and consent to participate

This study was approved by the Scientific Research Projects Approval Determination of Independent Ethics Committee of Hunan Xiangya Stomatological Hospital Central South University, affiliated with Central South University (Changsha, China). Written informed consent was obtained from all patients before the samples were collected during surgery.

Patient consent for publication

Not applicable.

Competing interests

The authors declare that they have no competing interests.

References

1. Yang PY, Chen YT, Wang YH, Su NY, Yu HC and Chang YC: Malignant transformation of oral submucous fibrosis in Taiwan: A nationwide population-based retrospective cohort study. J Oral Pathol Med 46: 1040-1045, 2017.
2. Pindborg JJ and Sirsat SM: Oral submucous fibrosis. Oral Surg Oral Med Oral Pathol 22: 764-779, 1966.
3. Shen YW, Shih YH, Fuh LJ and Shieh TM: Oral Submucous Fibrosis: A Review on Biomarkers, Pathogenic Mechanisms, and Treatments. Int J Mol Sci 21: 7231, 2020.
4. Arakeri G, Rai KK, Hunasgi S, Merkx MA, Gao S and Brennan PA: Oral submucous fibrosis: An update on current theories of pathogenesis. J Oral Pathol Med 46: 406-412, 2017.
5. Yoithapprabhunath TR, Maheswaran T, Dineshshankar J, Anusushanth A, Sindhuja P and Sitra G: Pathogenesis and therapeutic intervention of oral submucous fibrosis. J Pharm Bioallied Sci 5 (Suppl 1): S85-S88, 2013.
6. Hashimoto S, Gon Y, Takeshita I, Matsumoto K, Maruoka S and Horie T: Transforming growth Factor-beta1 induces phenotypic modulation of human lung fibroblasts to myofibroblast through a c-Jun-NH2-terminal kinase-dependent pathway. Am J Respir Crit Care Med 163: 152-157, 2001.
7. Wei Y, Kim TJ, Peng DH, Duan D, Gibbons DL, Yamauchi M, Jackson JR, Le Saux CJ, Calhoun C, Peters J, *et al*: Fibroblast-specific inhibition of TGF-β1 signaling attenuates lung and tumor fibrosis. J Clin Invest 127: 3675-3688, 2017.
8. Tilakaratne WM, Klinikowski MF, Saku T, Peters TJ and Warnakulasuriya S: Oral submucous fibrosis: Review on aetiology and pathogenesis. Oral Oncol 42: 561-568, 2006.
9. Rajalalitha P and Vali S: Molecular pathogenesis of oral submucous fibrosis - a collagen metabolic disorder. J Oral Pathol Med 34: 321-328, 2005.

10. Kale AD, Mane DR and Shukla D: Expression of transforming growth factor β and its correlation with lipodystrophy in oral submucous fibrosis: An immunohistochemical study. Med Oral Patol Oral Cir Bucal 18: e12-e18, 2013.
11. Pant I, Rao SG and Kondaiah P: Role of areca nut induced JNK/ATF2/Jun axis in the activation of TGF-β pathway in precancerous Oral Submucous Fibrosis. Sci Rep 6: 34314, 2016.
12. Hsieh YP, Chen HM, Lin HY, Yang H and Chang JZ: Epigallocatechin-3-gallate inhibits transforming-growth-factor-β1-induced collagen synthesis by suppressing early growth response-1 in human buccal mucosal fibroblasts. J Formos Med Assoc 116: 107-113, 2017.
13. Li J, Zhao TT, Zhang P, Xu CJ, Rong ZX, Yan ZY and Fang CY: Autophagy mediates oral submucous fibrosis. Exp Ther Med 11: 1859-1864, 2016.
14. Chang JZ, Yang WH, Deng YT, Chen HM and Kuo MY: EGCG blocks TGFβ1-induced CCN2 by suppressing JNK and p38 in buccal fibroblasts. Clin Oral Investig 17: 455-461, 2013.
15. Tkach M and Théry C: Communication by Extracellular Vesicles: Where We Are and Where We Need to Go. Cell 164: 1226-1232, 2016.
16. Hu Y, Rao SS, Wang ZX, Cao J, Tan YJ, Luo J, Li HM, Zhang WS, Chen CY and Xie H: Exosomes from human umbilical cord blood accelerate cutaneous wound healing through miR-21-3p-mediated promotion of angiogenesis and fibroblast function. Theranostics 8: 169-184, 2018.
17. Chen CY, Rao SS, Ren L, Hu XK, Tan YJ, Hu Y, Luo J, Liu YW, Yin H, Huang J, *et al*: Exosomal DMBT1 from human urine-derived stem cells facilitates diabetic wound repair by promoting angiogenesis. Theranostics 8: 1607-1623, 2018.
18. Sjoqvist S, Kasai Y, Shimura D, Ishikawa T, Ali N, Iwata T and Kanai N: Oral keratinocyte-derived exosomes regulate proliferation of fibroblasts and epithelial cells. Biochem Biophys Res Commun 514: 706-712, 2019.
19. Lou G, Yang Y, Liu F, Ye B, Chen Z, Zheng M and Liu Y: MiR-122 modification enhances the therapeutic efficacy of adipose tissue-derived mesenchymal stem cells against liver fibrosis. J Cell Mol Med 21: 2963-2973, 2017.
20. Qu Y, Zhang Q, Cai X, Li F, Ma Z, Xu M and Lu L: Exosomes derived from miR-181-5p-modified adipose-derived mesenchymal stem cells prevent liver fibrosis via autophagy activation. J Cell Mol Med 21: 2491-2502, 2017.
21. Zhu F, Chong Lee Shin OL, Pei G, Hu Z, Yang J, Zhu H, Wang M, Mou J, Sun J, Wang Y, *et al*: Adipose-derived mesenchymal stem cells employed exosomes to attenuate AKI-CKD transition through tubular epithelial cell dependent Sox9 activation. Oncotarget 8: 70707-70726, 2017.
22. Wang L, Hu L, Zhou X, Xiong Z, Zhang C, Shehada HM, Hu B, Song J and Chen L: Exosomes secreted by human adipose mesenchymal stem cells promote scarless cutaneous repair by regulating extracellular matrix remodelling. Sci Rep 7: 13321, 2017.
23. Khan I, Kumar N, Pant I, Narra S and Kondaiah P: Activation of TGF-β pathway by areca nut constituents: A possible cause of oral submucous fibrosis. PLoS One 7: e51806, 2012.
24. Yang SF, Hsieh YS, Tsai CH, Chen YJ and Chang YC: Increased plasminogen activator inhibitor-1/tissue type plasminogen activator ratio in oral submucous fibrosis. Oral Dis 13: 234-238, 2007.
25. Ni WF, Tsai CH, Yang SF and Chang YC: Elevated expression of NF-kappaB in oral submucous fibrosis - evidence for NF-kappaB induction by safrole in human buccal mucosal fibroblasts. Oral Oncol 43: 557-562, 2007.
26. Li X, Xie X, Lian W, Shi R, Han S, Zhang H, Lu L and Li M: Exosomes from adipose-derived stem cells overexpressing Nrf2 accelerate cutaneous wound healing by promoting vascularization in a diabetic foot ulcer rat model. Exp Mol Med 50: 1-14, 2018.
27. Han P, Lai A, Salomon C and Ivanovski S: Detection of salivary small extracellular vesicles associated inflammatory cytokines gene methylation in gingivitis. Int J Mol Sci 21: 5273, 2020.
28. Chomczynski P and Sacchi N: Single-step method of RNA isolation by acid guanidinium thiocyanate-phenol-chloroform extraction. Anal Biochem 162: 156-159, 1987.
29. Livak KJ and Schmittgen TD: Analysis of relative gene expression data using real time quantitative PCR and the 2 (Delta Delta C(T)) method. Methods 25: 402 408, 2001.
30. Rao AR and Das P: Evaluation of the carcinogenicity of different preparations of areca nut in mice. Int J Cancer 43: 728-732, 1989.
31. Gupta PC and Warnakulasuriya S: Global epidemiology of areca nut usage. Addict Biol 7: 77-83, 2002.
32. Cox SC and Walker DM: Oral submucous fibrosis. A review. Aust Dent J 41: 294-299, 1996.
33. Chang MC, Lin LD, Wu HL, Ho YS, Hsien HC, Wang TM, Jeng PY, Cheng RH, Hahn LJ and Jeng JH: Areca nut-induced buccal mucosa fibroblast contraction and its signaling: A potential role in oral submucous fibrosis - a precancer condition. Carcinogenesis 34: 1096-1104, 2013.
34. Chang YC, Tsai CH, Lai YL, Yu CC, Chi WY, Li JJ and Chang WW: Arecoline-induced myofibroblast transdifferentiation from human buccal mucosal fibroblasts is mediated by ZEB1. J Cell Mol Med 18: 698-708, 2014.
35. Kondaiah P, Pant I and Khan I: Molecular pathways regulated by areca nut in the etiopathogenesis of oral submucous fibrosis. Periodontol 2000 80: 213-224, 2019.
36. Han CY, Koo JH, Kim SH, Gardenghi S, Rivella S, Strnad P, Hwang SJ and Kim SG: Hepcidin inhibits Smad3 phosphorylation in hepatic stellate cells by impeding ferroportin-mediated regulation of Akt. Nat Commun 7: 13817, 2016.
37. Hu C, Dandapat A, Sun L, Khan JA, Liu Y, Hermonat PL and Mehta JL: Regulation of TGFbeta1-mediated collagen formation by LOX-1: Studies based on forced overexpression of TGFbeta1 in wild-type and lox-1 knock-out mouse cardiac fibroblasts. J Biol Chem 283: 10226-10231, 2008.
38. Sheppard D: Transforming growth factor beta: A central modulator of pulmonary and airway inflammation and fibrosis. Proc Am Thorac Soc 3: 413-417, 2006.
39. Angadi PV, Kale AD and Hallikerimath S: Evaluation of myofibroblasts in oral submucous fibrosis: Correlation with disease severity. J Oral Pathol Med 40: 208-213, 2011.
40. Wynn TA and Ramalingam TR: Mechanisms of fibrosis: Therapeutic translation for fibrotic disease. Nat Med 18: 1028-1040, 2012.
41. Dai JP, Zhu DX, Sheng JT, Chen XX, Li WZ, Wang GF, Li KS and Su Y: Inhibition of Tanshinone IIA, salvianolic acid A and salvianolic acid B on Areca nut extract-induced oral submucous fibrosis in vitro. Molecules 20: 6794-6807, 2015.
42. Teixeira FG, Carvalho MM, Sousa N and Salgado AJ: Mesenchymal stem cells secretome: A new paradigm for central nervous system regeneration? Cell Mol Life Sci 70: 3871-3882, 2013.
43. Xin H, Li Y and Chopp M: Exosomes/miRNAs as mediating cell-based therapy of stroke. Front Cell Neurosci 8: 377, 2014.
44. De Jong OG, Van Balkom BW, Schiffelers RM, Bouten CV and Verhaar MC: Extracellular vesicles: Potential roles in regenerative medicine. Front Immunol 5: 608-608, 2014.
45. Xie C, Ji N, Tang Z, Li J and Chen Q: The role of extracellular vesicles from different origin in the microenvironment of head and neck cancers. Mol Cancer 18: 83-83, 2019.
46. Sun X, Meng H, Wan W, Xie M and Wen C: Application potential of stem/progenitor cell-derived extracellular vesicles in renal diseases. Stem Cell Res Ther 10: 8-8, 2019.
47. Li FX, Liu JJ, Xu F, Lin X, Zhong JY, Wu F and Yuan LQ: Role of tumor-derived exosomes in bone metastasis. Oncol Lett 18: 3935-3945, 2019.
48. Valadi H, Ekström K, Bossios A, Sjöstrand M, Lee JJ and Lötvall JO: Exosome-mediated transfer of mRNAs and microRNAs is a novel mechanism of genetic exchange between cells. Nat Cell Biol 9: 654-659, 2007.
49. Illeperuma RP, Ryu MH, Kim KY, Tilakaratne WM and Kim J: Relationship of fibrosis and the expression of TGF-β1, MMP-1, and TIMP-1 with epithelial dysplasia in oral submucous fibrosis. Oral Med Pathol 15: 21-28, 2010.
50. Hu L, Wang J, Zhou X, Xiong Z, Zhao J, Yu R, Huang F, Zhang H and Chen L: Exosomes derived from human adipose mensenchymal stem cells accelerates cutaneous wound healing via optimizing the characteristics of fibroblasts. Sci Rep 6: 32993, 2016.
51. Cai Y, Li J, Jia C, He Y and Deng C: Therapeutic applications of adipose cell-free derivatives: A review. Stem Cell Res Ther 11: 312, 2020.
52. Li Y, Zhang W, Gao J, Liu J, Wang H, Li J, Yang X, He T, Guan H, Zheng Z, *et al*: Adipose tissue-derived stem cells suppress hypertrophic scar fibrosis via the p38/MAPK signaling pathway. Stem Cell Res Ther 7: 102, 2016.
53. Chai CY, Song J, Tan Z, Tai IC, Zhang C and Sun S: Adipose tissue-derived stem cells inhibit hypertrophic scar (HS) fibrosis via p38/MAPK pathway. J Cell Biochem 120: 4057-4064, 2019.